Published in final edited form as:
J Phys Chem B. 2009 April 9; 113(14): 4930–4939. doi:10.1021/jp810755p.

Does water relay play an important role in phosphoryl transfer reactions? Insights from theoretical study of a model reaction in water and *tert*-butanol

Yang Yang and **Qiang Cui***
Department of Chemistry and Theoretical Chemistry Institute, University of Wisconsin, Madison
1101 University Ave, Madison, WI 53706

Abstract

To investigate whether water relay plays an important role in phosphoryl transfer reactions, we have used several theoretical approaches to compare key properties of uridine 3'-m-nitrobenzyl phosphate (UNP) in the aqueous and *tert*-butanol solutions. Previous kinetic experiments found that the isomerization reaction of UNP is abolished in *tert*-butanol, which was interpreted as the direct evidence that supports the role of water relay in phosphoryl transfer. We have analyzed solute flexibility and solvent structure near the solute using equilibrium molecular dynamics simulations and a combined quantum mechanical/molecular mechanism (QM/MM) potential function for the solute. Snapshots from the simulations are then used in minimum energy path calculations to compare the energetics of direct nucleophilic attack and water-mediated nucleophilic attack pathways. QM/MM simulations are also used to compare the pseudo-rotation barriers for the pentavalent intermediate formed following the nucleophilic attack, another key step for the isomerization reaction. Combined results from these calculations suggest that water relay does not offer any significant energetic advantage over the direct nucleophilic attack. Unfortunately, the lack of isomerization in *tert*-butanol solution can not be straightforwardly explained based on the results we have obtained here and therefore requires additional analysis. This study, nevertheless, has provided new insights into several most commonly discussed possibilities.

1 Introduction

Phosphoryl transfer reactions are involved in many key biological processes such as energy transduction, signal transduction and protein/nucleic acids synthesis [1]. In additions, some RNA molecules have been found [2] to catalyze phosphoryl transfer reactions as well, and these ribozymes [3] have extended the definition of biological enzymes beyond protein systems, which stimulated the discussion of "RNA world" at the early stage of evolution [4]. The fundamental nature of phosphoryl transfer reactions has triggered an extensive body of experimental and theoretical analyses on their detailed mechanism [5–10]. It has been now established that the reaction pathway, such as being associative *vs*. dissociative [11–13] in nature, is likely sensitive to a number of factors that include pH, the pK_a values of the nucleophilic group and the leaving group as well as the presence of metal ions.

When the nucleophilic attack group has a relatively high pK_a, such as water or the 2'-OH group in RNA, it is commonly assumed that the biological phosphoryl transfer reaction has to be catalyzed by a general base [10]. The identity of the general base is often the question of interest and debate [9,14–18]. In some cases, no obvious base can be identified and it has been proposed

*To whom the correspondence should be addressed: E-mail: cui@chem.wisc.edu.

that the phosphate group may act as its own base and accept a proton from the nucleophile. An immediate example that led us to this problem is the hydrolysis of ATP in the molecular motor myosin [19], where the γ phosphate has been proposed to accept one proton from the nucleophilic water; the similar scenario has also been proposed for the hydrolysis of GTP in the signaling protein complex, Ras-GAP [14,16]. Moreover, as illustrated in Scheme 1, a direct proton transfer from the nucleophile (e.g., water or 2'-OH in RNA) to the phosphate group has been argued to be energetically unfavorable based on stereoelectronic consideration [10]: a four-centered transition state is expected to be high energy in nature. Therefore, it has been proposed that proton transfer proceeds through one or more "relay groups", which can be water molecule(s) (see Scheme 1) or amino acid sidechain(s), such that a less strained transition state is involved [10]. Specifically for ATP hydrolysis in myosin, high-resolution x-ray structure with the ATP hydrolysis transition state analogue, $ADP \cdot VO_4^-$, indicates that the sidechain of the conserved residue, Ser236, appears to be in an ideal position to relay the proton transfer [20]. However, somewhat surprisingly, mutation of Ser236 to an Alanine does not significantly perturb the hydrolysis activity [21]. Since the interpretation of mutagenesis results is not always straightforward, this result by itself does not imply that proton relay is not important for ATP hydrolysis in myosin; for example, it is possible that a water molecule in the mutant takes the place of the Ser236 sidechain in the WT enzyme, although preliminary calculations (Yang and Cui, work in progress) and recent X-ray crystallographic studies of the Ser236 mutant (Frye and Rayment, manuscript in preparation) do not support this possibility. Clearly, the potential complexity points to the value of analyzing the relevant model systems in solution.

In this context, a highly relevant model system is uridine 3'-m-nitrobenzyl phosphate (UNP), which has been studied in detail by Cleland and co-workers [22] to probe mechanistic issues concerning isomerization and cleavage reactions in RNA. Specifically, they studied the isomerization and cleavage reactions of UNP under different pH conditions in aqueous solution using kinetic isotope effects. It was proposed that under the neutral pH condition the isomerization reaction goes through a phosphorane-like pentavalent intermediate and that for this intermediate to form, water molecules are required to mediate the proton transfer from the 2'-hydroxyl group (proton donor) to the non-bridging oxygen of the phosphate moiety (proton acceptor, see Scheme 2). The proposal was tested by studying the same system in the anhydrous *tert*-butanol, and it was found that the isomerization reaction was abolished. Their explanation for this observation is that *tert*-butanol molecules are too bulky to insert between the proton donor and accepter groups, thus proton transfer is abolished, which in turn prevents the formation of the phosphorane-like intermediate and therefore the isomerization reaction. In other words, the difference between the reactivity in aqueous solution and the anhydrous *tert*-butanol seems to be the most direct evidence to date supporting the importance of proton relay in phosphoryl transfer reactions.

Theoretically, although relayed proton transfer can be energetically more favorable, the "catalytic" effect of relay can be significantly reduced when the entropic cost associated with constructing the relay pathway is taken into consideration. This is perhaps one of the reasons that the issue of relayed proton transfer in phosphoryl transfer reactions has not been analyzed extensively in previous computational analysis [5,23–25]. For the hydrolysis of monomethyl monophosphate ester (MMP), Burt et al. [26] did show that water relay plays an important role for the dissociative mechanism although their study did not address the entropic contribution. Moreover, in our recent study of mono/di-methyl monophosphate ester hydrolysis as part of our effort to develop effective approximate QM methods for phosphate chemistry [27], the role of the proton relay was found to be very modest even at the potential energy level for the associative mechanism. Therefore, from the limited number of theoretical analyses, it is not immediately obvious that proton relay is crucial to phosphoryl transfer reactions, and it is worthwhile to reanalyze the UNP reactivity and related problems using state-of-the-art computational methods.

In the current work, we use theoretical approaches to systematically analyze all the elementary steps in the UNP isomerization process. The results are used to evaluate the mechanistic basis behind the different reactivities in aqueous and *tert*-butanol solutions as observed experimentally [22]. Different simulation techniques are used to analyze the relevant steps individually. Specifically, we apply quantum mechanical/molecular mechanical (QM/MM) [28–30] molecular dynamics (MD) simulations to explore the structural flexibility of the solute and equilibrium solvent structures around the solute in both aqueous and *tert*-butanol solutions, especially concerning the number of solvent molecules that bridge the proton donor/acceptor groups. Based on the microscopic trajectories, cluster models with different numbers (0, 1) of solvent molecules between the proton donor/acceptor groups are studied using minimum energy path (MEP) calculations with high-level QM methods; the results provide quantitative clues regarding the dependence of proton transfer and phosphoryl transfer energetics on the solvent relay. Finally, pseudo-rotation [10,31] that links different critical conformations of the phosphorane-like intermediate is also characterized via potential of mean force simulations with a QM/MM potential.

The paper is organized as follows: details of the computational methods and system set-ups are summarized in Sect. 2; the results of simulations are presented in Sect. 3 and discussed in connection with experimental observations in Sect. 4; finally, conclusions are summarized in Sect. 5.

2 Computational Methods

The calculations in this study include both microscopic QM/MM simulations with explicit solvents and MEP calculations using cluster models with implicit solvent models. The QM/MM simulations are made possible by a recently parameterized approximate density functional theory, SCC-DFTBPR [27], which appear to have the proper balance between computational efficiency and accuracy for phosphate chemistry (mainly hydrolysis). These simulations are carried out using a local version of CHARMM [32]. The MEP calculations are done using density functional theory [33] with snapshots from QM/MM trajectories; they are carried out with the Gaussian03 package [34].

2.1 Equilibrium QM/MM simulations

In both aqueous and *tert*-butanol solutions, the solute molecule, “UNP”, is treated quantum mechanically and all solvent molecules are described using TIP3P for water [35] and a newly developed force field for *tert*-butanol (see below). For computational efficiency, the solute UNP is simplified by replacing the m-nitrobenzyl group by a hydrogen and replacing the uracil group by NH_2 (see Fig.1); the net charge of the solute is −1, consistent with the pH neutral condition in the experimental study [22]. In the subsequent discussions, we refer the solute simply as UNP for convenience.

For the aqueous solution simulations, UNP is solvated with a water droplet of 22 Å radius; for the *tert*-butanol solution simulations, the solute is solvated by a droplet of 25 Å radius. The generalized solvent boundary potential (GSBP) approach [36,37] is applied as the boundary condition, where the bulk dielectric constant is taken to be 80.0 and 8.22 for water and *tert*-butanol, respectively. The SHAKE algorithm [38] is used to constrain all bonds involving hydrogen, which makes it possible to use an integration time step of 1 fs. Two independent sets of 300ps simulations are performed for both solutions, and the last 100ps data in each trajectory are used for analysis. Aqueous solution is studied under the room temperature (298K), and the *tert*-butanol solution is investigated at 330K due to the high melting point of *tert*-butanol (the normal melting point is 298.8K [39]); we note that the experimental study in Ref. [22] was carried out at 86° for both solutions.

The MM parameters for *tert*-butanol are based on the most similar molecule (2-propanol) in the CHARMM27 force field [40], with slight variations in partial charges within the CHARMM convention (i.e., replacing the non-polar H in 2-propanol with a methyl group, then adjusting the partial charges on the central carbon such that the net charge of the molecule is zero). As shown in the Supporting Materials, the MM parameters lead to properties for pure *tert*-butanol, including number density, heat of vaporization and self-diffusion coefficient, in good agreement with available experimental data [39].

To have a reliable description of solute-solvent interactions, van der Waals parameters for five critical oxygen atoms of UNP (O_7, O_8, O_{11}, O_{12} and O_{14} as labeled in Fig.1) have been optimized for the SCC-DRTBPR model following the standard protocol [41]. Specifically, 48 gas-phase bimolecular (UNP-water) interaction potential energy curves (273 data points) at the B3LYP [42–44]/6–31+G** [45–48] level are used as reference to optimize the van der Waals parameters using a Genetic Algorithm (micro-GA) approach [49]. The optimized van der Waals parameters (see Supporting Information) give a root-mean-square-error (RMSE) of 1.7 kcal/mol for the B3LYP reference interaction energies.

2.2 Minimum energy path (MEP) analysis for phosphoryl transfer

Since the main goal of this work is to explore the importance of water relay in phosphoryl transfer reactions, MEP calculations have been carried out starting from snapshots from QM/MM trajectories that include either no water between the donor and acceptor groups (“direct-attack” mechanism) or a single water as the potential proton relay (“proton-relay” mechanism). To explore the impact of thermal fluctuations, nine snapshots are taken for the “direct-attack” pathway and seven snapshots are used for the “water-relay” pathway. Longer solvent bridges are deemed less important based on the statistics collected from equilibrium QM/MM simulations (see discussions below in Sect.3.1).

For computational efficiency, the snapshots are first fully optimized at the SCC-DFTBPR level in the gas phase, which are then used as starting points for MEP calculations based on the conjugate peak refinement algorithm implemented in CHARMM [50]. The SCC-DFTBPR results are in turn used as the initial guess for obtaining optimized stationary points (reactant, transition state and intermediate) at the B3LYP/6–31+G* level; frequency calculations are carried out to estimate the zero-point energy and thermal corrections at 298.15K. For better energetics, single point energy calculations are done using the larger 6–311++G** basis set [46,51], with the solvation effect taken into consideration with the polarizable continuum model (PCM) [52]. To explore the sensitivity of the PCM results to the choice of parameters, the solvation calculations are done with both the United Atom Kohn Sham (UAKS) radii and the Pauling radii that define the solute cavity [53]. The SCC-DFTBPR results are largely consistent with the B3LYP results in the gas-phase, thus only the B3LYP results are discussed below. Regarding the reliability of the B3LYP results, we note that our recent studies [27] have compared B3LYP and MP2 calculations with large basis sets (e.g., those used in the G2/G3 calculations [54,55]) for very similar phosphoryl transfer reactions, including the possible involvement of water relays. The results at the B3LYP and MP2 levels are very consistent, especially for the mono-anionic systems; for example, the root-mean-square-difference is 2.5 kcal/mol for 37 reaction energies. Further considering that we are focusing on the role of the water relay on the energy barriers, the B3LYP approach ought to be a valid method of choice here.

2.3 Pseudo-rotation potential of mean force (PMF)

To evaluate whether pseudo-rotation in the phosphorane-like intermediate may have significantly different energetics in aqueous and *tert*-butanol solutions, PMF calculations have been carried out for both cases using the SCC-DFTBPR/MM protocol as described above. The

reaction coordinate for characterizing the pseudo-rotation is defined as a linear combination of O_7-O_{12} and O_8-O_{11} distances, i.e., $d(O_7\text{-}O_{12})$-$d(O_8\text{-}O_{11})$. This combination is linearly correlated to the expected pseudo-rotation motion (i.e., O_7-P-O_{12} angle compresses and O_8-P-O_{11} angle expands simultaneously, see Fig.S2 in Supporting Information) throughout the umbrella sampling simulations [56], indicating that the reaction coordinate is valid. For the *tert*-butanol solution, 15 windows are employed with 50 ps simulation for each window; for the aqueous solution, 19 windows are used with also 50 ps sampling for each window. The harmonic force constant for the umbrella potential is 500 kcal/(mol·$Å^2$). To be consistent with the equilibrium simulations, the PMF calculations are done at 330 K and 298 K for the *tert*-butanol and aqueous solution, respectively. The Weighted Histogram Analysis Method (WHAM) [57] is employed to produce the one-dimensional PMF based on the statistics of the reaction coordinate recorded at each step of the last 20 ps in each window.

3 Results

3.1 Solute flexibility and solvent distribution from equilibrium QM/MM simulations

First, we compare the structural flexibility of the solute (UNP) and solvent distribution in aqueous and *tert*-butanol solutions based on equilibrium QM/MM simulations.

3.1.1 Aqueous Solution—In the aqueous solution, the general observation is that the solute is structurally flexible and may adopt a broad range of conformations that interconvert rapidly at the picosecond time scale. As a result, the solvent distribution around the key oxygen atoms (Fig.2) converges quickly and does not vary much when a different initial structure for the solute is used. The solvent distributions follow the expected trend that the level of solvation is higher around the more negatively charged phosphoryl oxygen atoms (O_{11}, O_{14}, see Fig.1 for notation), which indicates the lack of persistent intra-solute hydrogen bonding (see below for the *tert*-butanol case). Snapshots from the trajectories (Fig.3) indeed capture very different orientations of the 2'-OH, the 5'-OH and the 3'-phosphate-ester groups. As shown in Fig.4, a few key geometrical parameters of the solute, such as the dihedral angles that characterize the orientation of the 3'-phosphate-ester group and the 5'-OH, undergo significant fluctuations even at the picosecond time scale. The nucleophilic attack distance between O_7 in the 2'-OH and the phosphorus atom fluctuates between 3.0 Å and 4.5 Å, which is likely correlated with the number of solvent molecules that bridge the two groups (see Fig.4 for several scenarios). A more quantitative analysis of the hydrogen bonding pattern between the proton donor (2'-OH) and acceptor (3'-phosphate-ester group) is shown in Fig.5, following the similar protocol used in our analysis of long-range proton transfer in carbonic anhydrase [58,59]; note that since we are interested in proton transfer from the 2'-OH group, we consider only those hydrogen bonding interactions where the 2'-OH serves as the hydrogen donor. In most cases (>70%), there is actually not any well-defined hydrogen bonding interaction between the donor/acceptor groups, since they are both well solvated by the water molecules and the 2'-OH points away from the phosphate group. In 10% of the trajectory frames, the donor and acceptor groups are involved in a direct hydrogen bond, and there is also similar levels of probability to have one or two water molecules that bridge the donor and acceptor groups; longer water wires occur with extremely low probabilities.

3.1.2 *tert*-butanol Solution—The behavior in the *tert*-butanol solution is quite different from that in the aqueous solution in that the solute tends to form intra-solute hydrogen bonds and thus is substantially less flexible. As shown in Fig.6, the solvent distributions from two independent simulations differ quite substantially, which indicates rather different solute structures that do not interconvert during the ~300ps simulation time for each trajectory. Indeed, snapshots from these trajectories illustrate different intramolecular hydrogen bonds that persist throughout the simulations. In one trajectory (Fig.7), a stable hydrogen bond is

formed between O_{11} of the phosphate to the 5'-OH; at the same time, a *tert*-butanol solvent is inserted between the phosphate and the 2'-OH, which is correlated with a long nucleophilic distance that fluctuates between 3.6 to 4.3 Å. In the other trajectory (Fig.8), a direct hydrogen bond is formed between O_{11} of the phosphate and the 2'-OH, leading to a shorter nucleophilic attack distance that fluctuates around 3.3 Å. In both cases, the fluctuations in the dihedral angle that characterizes the phosphate-ester group orientation are notably smaller than those observed for the aqueous solution (compare Fig.7–Fig.8 to Fig.4). The observation of intra-solute hydrogen bond in the *tert*-butanol simulations is consistent with the notion that it is a less polar and therefore less stabilizing solvent than water.

3.2 Barrier of phosphoryl transfer with and without water relay

The equilibrium simulations presented above illustrate that the two most relevant types of configurations for the phosphoryl transfer would involve either a direct hydrogen bonding between the 2'-OH and the phosphate group, or, in the case of aqueous solution, a water that potentially mediates the proton transfer. Although we do observe a *tert*-butanol solvent bridging the 2'-OH and the phosphate group (see Fig.7), we do not believe it is relevant for the reaction because the nucleophilic distance is too long (average ~ 4Å) due to the bulky size of *tert*-butanol; for the same reason, we do not consider the two-water-bridging cases despite their similar population as the single-water-bridge configurations (Fig.5). Therefore, we focus on two types of MEP calculations below: a direct nucleophilic attack mechanism without explicitly involving any solvent and the single-water-mediated nucleophilic attack mechanism.

3.2.1 Direct Nucleophilic Attack—As shown in Table 1, although there is notable differences between the overall conformation of the different initial structures (the root-mean-square-difference between different initial structures is about 1.25 Å), there is only small variation in the critical geometrical parameters, including those for the transition state. In the transition state, the distance between the nucleophilic oxygen and phosphorus decreases from ~3.4 Å in the reactant state to ~2.3 Å, and the nucleophilic attack angle is close to be 162°. The proton transfer from the 2'-OH to the phosphate group has essentially completed as indicated by the short distance of ~0.99 Å for the proton/phosphate separation (H_{22}-$O_{11/14}$) in the transition state.

As to the energetics, which are summarized in Table 2, the reaction is highly endothermic in the gas-phase by about 28–29 kcal/mol; including the zero-point and thermal corrections does not change the value significantly. The barrier height is about 30 kcal/mol and decreases by ~ 1 kcal/mol with zero-point and thermal corrections. Including the solvation effect (in water) using the PCM model also leads to only minor changes and the results depend a bit on the set of radii used; with the UAKS radii, the best estimate for the free energy barrier is ~25 kcal/mol, while it is ~27 kcal/mol with the Pauling radii. With a simple transition state theory estimate and assuming that this step is rate limiting, the rate constant is ~2.9×10^{-4} s^{-1} at at 86 °C, which is in fact higher compared to the experimental value of Cleland and co-workers (~ ~6.0×10^{-7} s^{-1}) under neutral pH (and 86°) [22].

3.2.2 Single-water-mediated nucleophilic attack—With one water molecule bridging the 2'-OH and the phosphate group, the nucleophilic attack distance is longer in both the reactant and transition state compared to the direct nucleophilic attack mechanism; the values are ~4.1 Å and 2.9 Å in the reactant and transition state, respectively, as compared to the values of ~3.4 Å and ~2.3 Å, respectively, in the direct attack mechanism. The nucleophilic attack angle is also slightly further away from linearity, ~ 156° vs. ~ 162° in the direct attack mechanism, although there is a notable standard deviation of ~4° (Table 1). The relayed proton transfers are also essentially completed in the transition states, as judged by the relevant proton-oxygen distances (Table 1).

Concerning the energetics, it is interesting that involving the water relay has a very minor impact on both the endothermicity and barrier height. For example, the best estimate of the barrier is ~24 kcal/mol with the UAKS radii and ~25 kcal/mol with the Pauling radii; both only differ from the direct attack results by ~ 1–2 kcal/mol. Therefore, the current calculations show that water relay does not have any major energetic impact on the phosphoryl transfer in the (model) UNP system (see further discussions below in Sect.4).

3.3 Energetics of pseudo-rotation of the pentavalent intermediate in water and *tert*-butanol solutions

As shown in Fig.9, the pseudo-rotations in water and *tert*-butanol solution have very similar energetics with a free energy barrier ~ 5–6 kcal/mol; in the transition state, the expansion angle (between O_8-P-O_{11}) and the compression angle (between O_7-P-O_{12}) are also similar for the two cases, with both angles ~150° in water and ~140° in *tert*-butanol. Apparently, the larger size of *tert*-butanol does not have a major impact on the pseudo-rotation process, which is consistent with the observation that pseudo-rotation can proceed without any large scale swing of the phosphorus ligands. The barrier of ~5–6 kcal/mol in water is close to implicit solvent calculations of similar phosphate species [60,61].

4 Discussions

In the experimental study of Cleland and coworkers [22], whether water molecules are explicitly involved in the isomerization and cleavage reactions of UNP has been addressed by comparing the reactivity in aqueous and anhydrous *tert*-butanol solutions. The observation that the isomerization reaction was abolished in the *tert*-butanol solution was taken as the evidence for supporting the role of water in mediating the proton transfer from the 2'-OH to the phosphate group during the nucleophilic attack. We note that the isomerization from UNP to uridine 2'-m-nitrobenzyl phosphate involves several elementary steps, and, in principle, changes in any one of them could be the reason for abolishing the isomerization reaction in the *tert*-butanol solution. Therefore, to reach a reliable explanation for the experimental observation, all relevant solute properties and processes should be compared systematically for aqueous and *tert*-butanol solutions. In the current work, we have attempted to address the problem from a theoretical point of view, which include comparing the following properties in aqueous and *tert*-butanol solutions: the solute (UNP) flexibility and solute-solvent structure, nucleophilic attack reaction energetics, and pseudo-rotation that links different conformations of the intermediate state.

First, we consider the solute flexibility and solute-solvent structure at equilibrium. Whether a chemical reaction occurs readily is critically dependent on the accessibility (population) of reactant structures that are suitable for reaction. In the aqueous solution, the solute is found very flexible and quickly interconverts among different conformations at the picosecond time scale. Based on two independent ~300 ps simulations, the solute and solute/solvent configurations that satisfy either the direct-attack mechanism or the single-water-mediated mechanism account for more than 20% of the population (Fig.5), which is very significant. In the *tert*-butanol solution, by contrast, the solute is found to be much more rigid due to the higher tendency of forming intra-solute hydrogen bond(s). With a hydrogen-bond between 5'-OH and the phosphate group, the distance between the 2'-OH and phosphate tends to be too long for an effective nucleophilic attack, especially with a bulky *tert*-butanol inserted in between (Fig. 7). However, an alternative configuration that dominates the other trajectory involves a stable hydrogen bond between 2'-OH and phosphate (Fig.8), which seems ideal for a direct nucleophilic attack. To gain a rough estimate on the relative population of the two sets of solute configurations, we have optimized these two configurations using B3LYP/6–31++G** in the gas phase, followed by PCM single point calculations ($\epsilon_{tert-butanol}$=8.22); with the Pauling

radii, the configuration with the 5'-OH-phosphate hydrogen bond is more stable by ~1.5 kcal/mol, which corresponds to ~10 times higher in population. Therefore, the solute configuration that favors the direct-attack mechanism in *tert*-butanol is likely low (<10%) although this factor by itself is unlikely sufficient for completely abolishing the reactivity.

The observed trends in solute configuration and solvent structure might be able to explain the reactivity difference in aqueous and *tert*-butanol solutions if one argues that the nucleophilic attack barrier is substantially higher for the direct-attack mechanism than the single-water mediated mechanism; this is because the direct-attack mechanism is expected to be the only relevant pathway in *tert*-butanol solution, where the nucleophilic attack distance is too longer with a *tert*-butanol solvent inserted between the 2'-OH and phosphate groups. According to the stereoelectronic argument commonly employed in the literature [10,20], the water-mediate nucleophilic attack is indeed expected to be energetically more favorable than the direct attack mechanism. However, the MEP calculations performed here using different initial starting structures consistently find that there is a very small (<1–2 kcal/mol) energetic difference between the direct-attack and water-mediated pathways, and both barriers correlate well with the experimental rate constants under neutral pH [22]. This result can be explained by the fact that the proton transfer from 2'-OH to the phosphate group has largely completed in the transition state of both pathways, thus the magnitude of unfavorable steric interaction in the direct-attack pathway is unlikely significant at all. Moreover, the nucleophilic attack distance is substantially longer in the water-mediated (~2.9 Å) pathway than in the direct-attack (~2.3 Å) pathway, thus the weaker P-O interaction may have abolished any stereoelectronic advantage of the water-mediated transition state.

Finally, to complete the isomerization reaction from the penta-valent intermediate, the O_8-P bond needs to break. According to Westheimer's rule [31], the leaving group can only be cleaved at the axial position, which means a pseudo-rotation has to occur prior to P-O cleavage. The rate of pseudo-rotation is affected by various factors that include the degree of esterification, ligand structures (acyclic vs. cyclic), protonation state, solvation, although in general the barrier is expected to be low. For example, the pseudo-rotation barrier between P(O-)(OH)(-O-CH_2CH_2-O-)(OCH_3) and P(O-)(OCH_3)(-O-CH_2CH_2-O-)(OH) is calculated [60,61] to be 5.3 kcal/mol in the gas phase and ~2.6–2.8 kcal/mol in solution with PCM models. Considering the structural similarity of this molecule to UNP, it is reasonable to expect that the pseudo-rotation barrier in our system is also low, at least in the aqueous solution. In the *tert*-butanol solution, however, considering the bulky size of the solvent, a higher barrier might be expected, which motivated our PMF simulations with explicit solvents. However, as the PMF calculations (Fig.9) indicate, the pseudo-rotation of the penta-valent intermediate has comparable barriers in the aqueous and *tert*-butanol solutions, which is consistent with the observation that the pseudo-rotation, in fact, involves fairly modest structural changes in the solute.

In summary, among all the key properties that we or others have speculated to be essential for an efficient phosphoryl transfer reaction, no major trend is observed that can straightforwardly explain the abolishment of UNP isomerization in the anhydrous *tert*-butanol solution. The solute is structurally much more rigid in *tert*-butanol due to the fact that the bulky *tert*-butanol is a worse solvent than water and therefore promotes intra-solute hydrogen bonds. Nevertheless, the 2'-OH and phosphate do not appear to have trouble forming a hydrogen bond that permits a direct nucleophilic attack mechanism. More importantly, unlike commonly assumed [10], the direct nucleophilic attack pathway has very similar energetics compared to a water mediated pathway, thus water relay does not seem to be essential in the phosphoryl transfer studied here. The pseudo-rotation barrier is also similar in the aqueous and *tert*-butanol solutions. Therefore, we have to conclude that the lack of UNP isomerization in the anhydrous

tert-butanol solution alone does not directly support the role of water relay in phosphoryl transfer reactions and some other reason(s) must be responsible for this observation.

5 Conclusions

Phosphoryl transfer reactions are fundamentally important in life processes. Their mechanism in the biological context is complex and therefore solution models are potentially useful for sorting out some mechanistic issues. One issue that has been discussed rather extensively is whether a relay group, which can be a water solvent or an amino acid in the enzyme active site, is required to facilitate the proton transfer from the nucleophilic group to the general base; the latter can be the phosphate group itself. The involvement of the relay group was motivated by stereoelectronic arguments, although an entropic consideration might render it less favorable especially in solution. The most relevant experimental data that we are aware of come from the study of the UNP system [22], where the key finding is that the isomerization reaction of UNP is abolished as the solvent changes from water to anhydrous *tert*-butanol; this has been interpreted as the direct support for the role of water relay in the phosphoryl transfer. By analyzing several relevant steps of UNP isomerization using a combination of theoretical studies, however, we show that this interpretation is not as straightforward as originally thought. QM/MM simulations show that in both aqueous and *tert*-butanol solutions, the UNP molecule have a significant population for configurations in which the 2'-OH and the phosphate group are well oriented for a direct nucleophilic attack, while the single-water-mediated configuration is equally likely in the aqueous solution. However, MEP calculations show that both mechanisms have, in fact, very similar energetics; i.e., with an associative nature transition state, water relay does not have any advantage even without invoking entropic considerations. Therefore, the lack of isomerization in UNP alone can not be used as a clear evidence for supporting the role of water relay in phosphoryl transfer reactions. Unfortunately, the precise reason for this interesting experimental observation remains unclear after this study, although we have been able to provide new insights into several most commonly discussed possibilities.

Supplementary Material

Refer to Web version on PubMed Central for supplementary material.

Acknowledgments

The research discussed here has been supported from the National Institutes of Health (R01-GM071428). Q.C. also acknowledges a Research Fellowship from the Alfred P. Sloan Foundation. Computational resources from the National Center for Supercomputing Applications at the University of Illinois are greatly appreciated.

References and Notes

1. Alberts, B.; Bray, D.; Lewis, J.; Raff, M.; Roberts, K.; Watson, JD. Molecular biology of the cell. Garland Publishing, Inc; 1994.
2. Cech TR, Bass BL. Ann. Rev. Biochem 1986;55:599–629. [PubMed: 2427016]
3. Doherty EA, Doudna JA. Annu. Rev. Biophys. Biomol. Struct 2001;30:457–475. [PubMed: 11441810]
4. Gilbert W. Nature 1986;319:618, 618.
5. Florian J, Warshel A. J. Phys. Chem. B 1998;102:719–734.
6. Åqvist J, Kolmodin K, Florian J, Warshel A. Chem. Biol 1999;6:R71–R80. [PubMed: 10074472]
7. Herschlag D, Jencks WP. J. Am. Chem. Soc 1989;111:7579–7586.
8. Admiraal SJ, Herschlag D. J. Am. Chem. Soc 2000;122:2145–2148.
9. Narlikar GJ, Herschlag D. Ann. Rev. Biochem 1997;66:19–59. [PubMed: 9242901]
10. Cleland WW, Hengge AC. Chem. Rev 2006;106:3252–3278. [PubMed: 16895327]
11. Guthrie RD, Jencks WP. Acc. Chem. Res 1989;22:343–349.

12. Hassett A, Blättler W, Knowles JR. Biochem 1982;21:6335–6340. [PubMed: 7150563]
13. Kamerlin SCL, Florian J, Warshel A. ChemPhysChem 2008;9:1767–1773. [PubMed: 18666265]
14. Mildvan AS. Proteins: Struct., Funct., and Genet 1997;29:401–416. [PubMed: 9408938]
15. Langen R, Schweins T, Warshel A. Biochem 1992;31:8691–8696. [PubMed: 1390653]
16. Glennon TM, Villa J, Warshel A. Biochem 2000;39:9641–9651. [PubMed: 10933780]
17. Lee TS, York DM. J. Am. Chem. Soc 2008;130:7168–7169. [PubMed: 18479101]
18. Nam K, Gao JL, York DM. RNA 2008;14:1501–1507. [PubMed: 18566190]
19. Rayment I. J. Biol. Chem 1996;271:15850–15853. [PubMed: 8663496]
20. Smith CA, Rayment I. Biochemistry 1996;35:5404–5417. [PubMed: 8611530]
21. Shimada T, Sasaki N, Ohkura R, Sutoh K. Biochem 1997;36:14037–14043. [PubMed: 9369475]
22. Gerratana B, Sowa GA, Cleland WW. J. Am. Chem. Soc 2000;122:12615–12621.
23. Klahn M, Rosta E, Warshel A. J. Am. Chem. Soc 2006;128:15310–15323. [PubMed: 17117884]
24. Lopez X, Dejaegere A, Leclerc F, York DM, Karplus M. J. Phys. Chem. B 2006;110:11525–11539. [PubMed: 16771429]
25. Nam KH, Gao JL, York DM. J. Am. Chem. Soc 2008;130:4680–4691. [PubMed: 18345664]
26. Wang Y, Topol IA, Collins JR, Burt SK. J. Am. Chem. Soc. 2005
27. Yang Y, Yu H, York DM, Elstner M, Cui Q. J. Chem. Theo. Comp 2008;4:2067–2084.
28. Field MJ, Bash PA, Karplus M. J. Comput. Chem 1990;11(6):700–733.
29. Gao J, Truhlar DG. Annu. Rev. Phys. Chem 2002;53:467. [PubMed: 11972016]
30. Warshel A. Annu. Rev. Biophys. Biomol. Struct 2003;32:425–443. [PubMed: 12574064]
31. Westheim FH. Acc. Chem. Res 1968;1:70.
32. Brooks BR, Bruccoleri RE, Olafson BD, States DJ, Swaminathan S, Karplus M. J. Comput. Chem 1983;4(2):187–217.
33. Parr, RG.; Yang, WT. Density-Functional Theory of Atoms and Molecules. New York: Oxford University Press; 1989.
34. Gaussian 03, Revision B.05. Frisch, M. J. et al., and Pople, J.A.. 2003.
35. Jorgensen WL, Chandrasekhar J, Madura JD, Impey RW, Klein ML. J. Chem. Phys 1983;79(2):926–935.
36. Im W, Bernéche S, Roux B. J. Chem. Phys 2001;114(7):2924–2937.
37. Schaefer P, Riccardi D, Cui Q. J. Chem. Phys 2005;123014905
38. Ryckaert J-P, Ciccotti G, Berendsen HJC. J. Comput. Phys 1977;23(3):327–341.
39. Lide, DR., editor. CRC Handbook Chemistry and Physics. Vol. 85 ed.. CRC Press; 2005.
40. MacKerell AD Jr, Karplus M, et al. J. Phys. Chem. B 1998;102:3586–3616.
41. Riccardi D, Li G, Cui Q. J. Phys. Chem. B 2004;108:6467–6478. [PubMed: 18950136]
42. Becke AD. Phys. Rev. A 1988;38:3098–3100. [PubMed: 9900728]
43. Becke AD. J. Chem. Phys 1993;98:5648–5652.
44. Lee C, Yang W, Parr RG. Phys. Rev. B 1988;37:785–789.
45. Haharan PC, Pople JA. Theor. Chim. Acta 1973;28:213–222.
46. Krishnan R, Binkley JS, Seeger R, Pople JA. j. Chem. Phys 1980;72:650–654.
47. Frisch MJ, Pople JA, Binkley JS. J. Chem. Phys 1984;80:3265–3269.
48. Clark T, Chandrasekhar J, Spitznagel GW, vR Schleyer P. J. Comp. Chem 1983;4:294–301.
49. Goldberg, DE. Genetic Algorithms in Search, Optimization, and Machine Learning. Boston: Addison-Wesley; 1989.
50. Fischer S, Karplus M. Chem. Phys. Lett 1992;194:252–261.
51. McLean AD, Chandler GS. J. Chem. Phys 1980;72:5639–5648.
52. Cossi M, Barone V, Cammi R, Tomasi J. Chem. Phys. Lett 1996;255:327–335.
53. Barone V, Cossi M, Tomasi J. J. Chem. Phys 1997;107:3210–3221.
54. Curtiss LA, Raghavachari K, Pople JA. J. Chem. Phys 1995;103:4192–4200.
55. Curtiss LA, Raghavachari K, Redfern PC, Rassolov V, Pople JA. J. Chem. Phys 1998;109:7764–7776.

56. Torrie G, Valleau J. J. Comp. Phys 1977;23:187–199.
57. Kumar S, Bouzida D, Swendsen RH, Kollman PA, Rosenberg JM. J. Comput. Chem 1992;13(8): 1011–1021.
58. Riccardi D, Schaefer P, Yang Y, Yu H, Ghosh N, Prat-Resina X, König P, Xu D, Guo H, Elstner M, Cui Q. J. Phys. Chem. B 2006;110(13):6458–6469. [PubMed: 16570942]
59. Riccardi D, Koenig P, Guo H, Cui Q. Biochem 2008;47:2369–2378. [PubMed: 18247480]
60. Lopez CS, Faza AN, Gregersen BA, Lopez X, de Lera AR, York DM. ChemPhysChem 2004;5:1045–1049. [PubMed: 15298394]
61. Lopez CS, Faza ON, de Lera AR, York DM. Chem. Eur. J 2005;11:2081–2093.
62. Humphrey W, Dalke A, Schulten K. J. Mol. Graph 1996;14:33–38. [PubMed: 8744570]

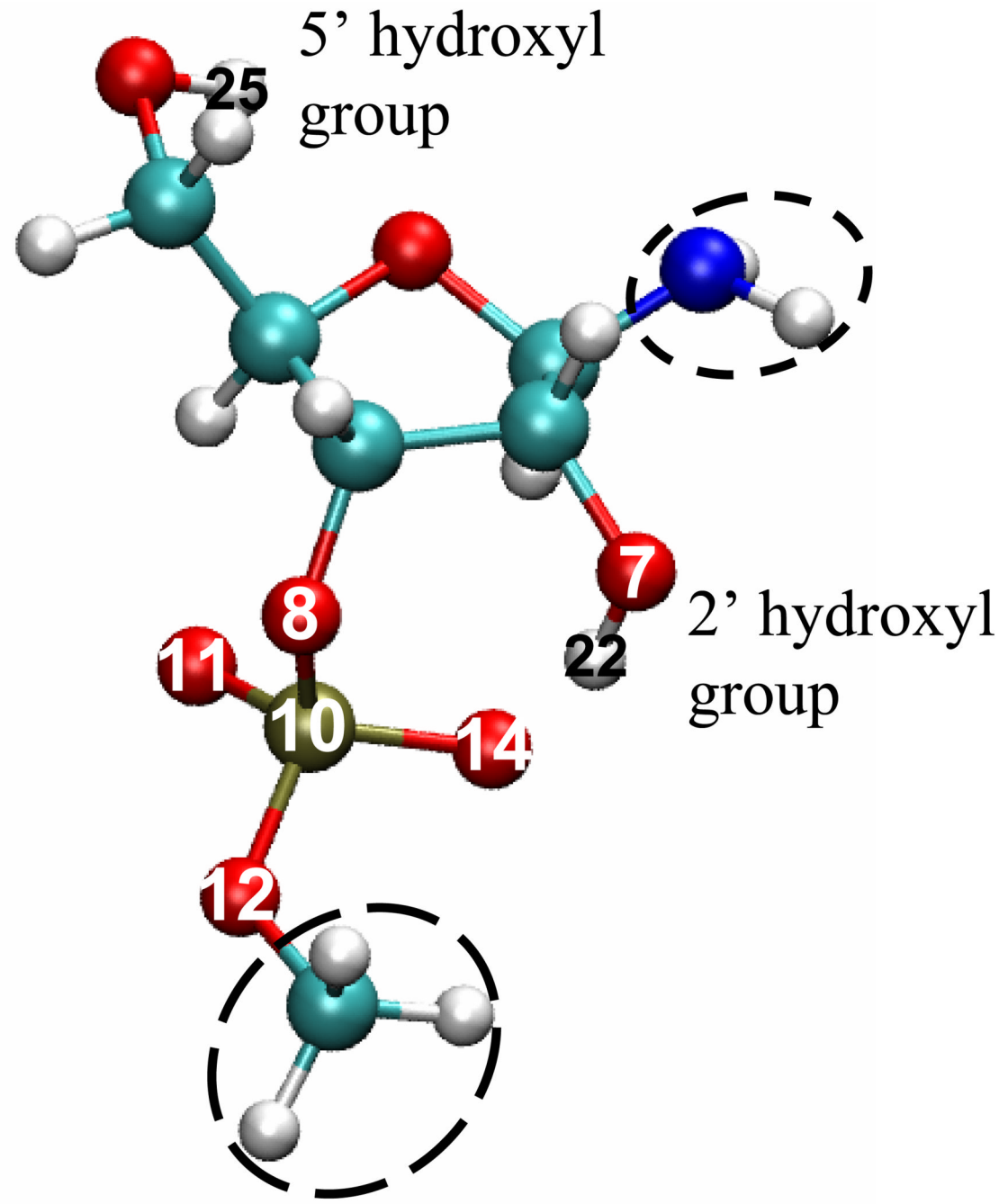

Figure 1.
The model structure for uridine 3’-m-nitrobenzyl phosphate (UNP) used in the current simulation study. The simplified moeities compared to the original solute are indicated by the circles. Atoms referred to in the discussions are labeled; the color scheme used for atoms is: oxygen in red, nitrogen in blue, carbon in cyan, hydrogen in white and phosphorus in gold. The figure is generated using VMD [62].

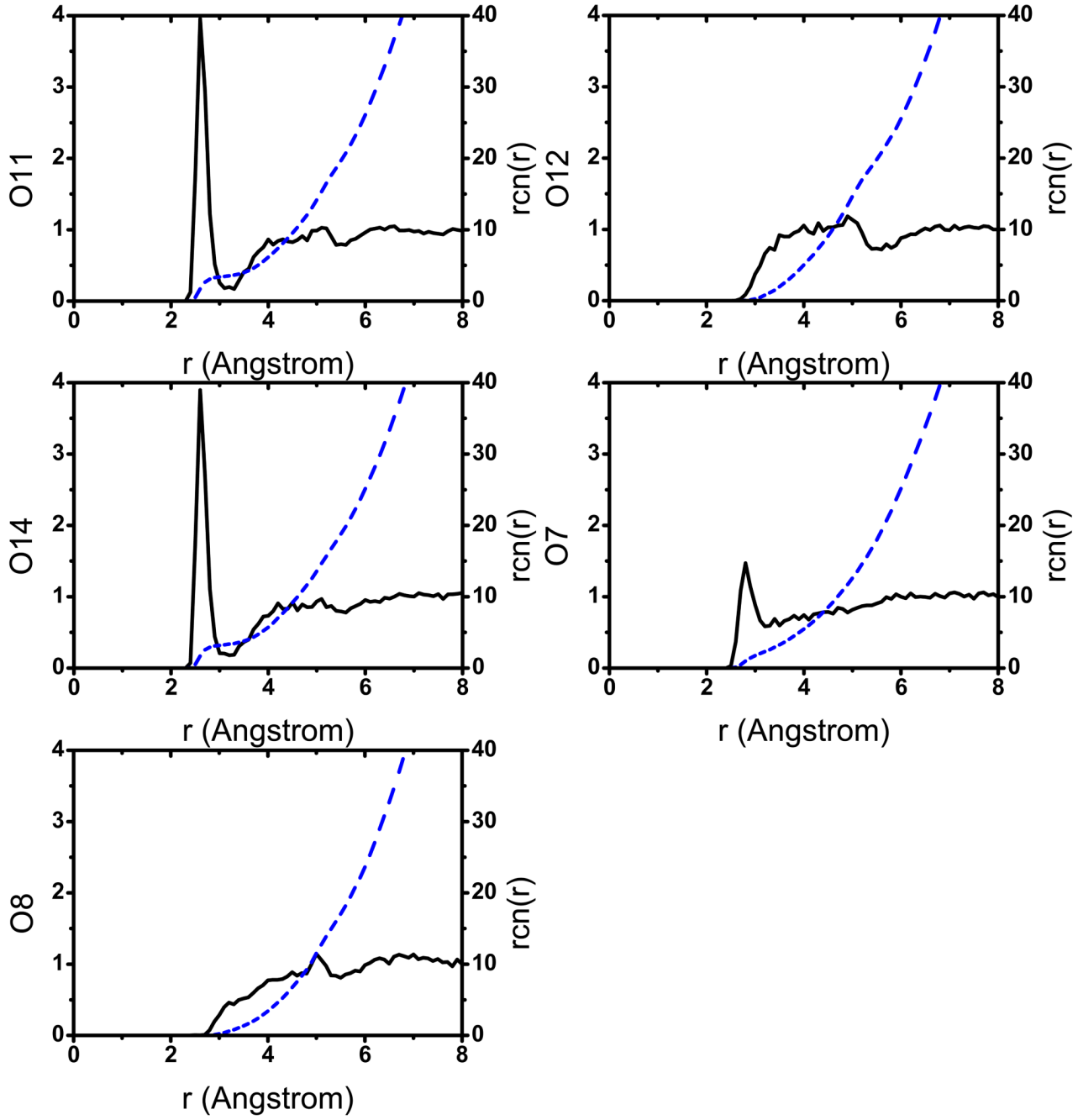

Figure 2.
Radial distribution functions, g(r) (solid lines) and running coordination numbers, rcn (dash lines), of water oxygen around different oxygen atoms of UNP.

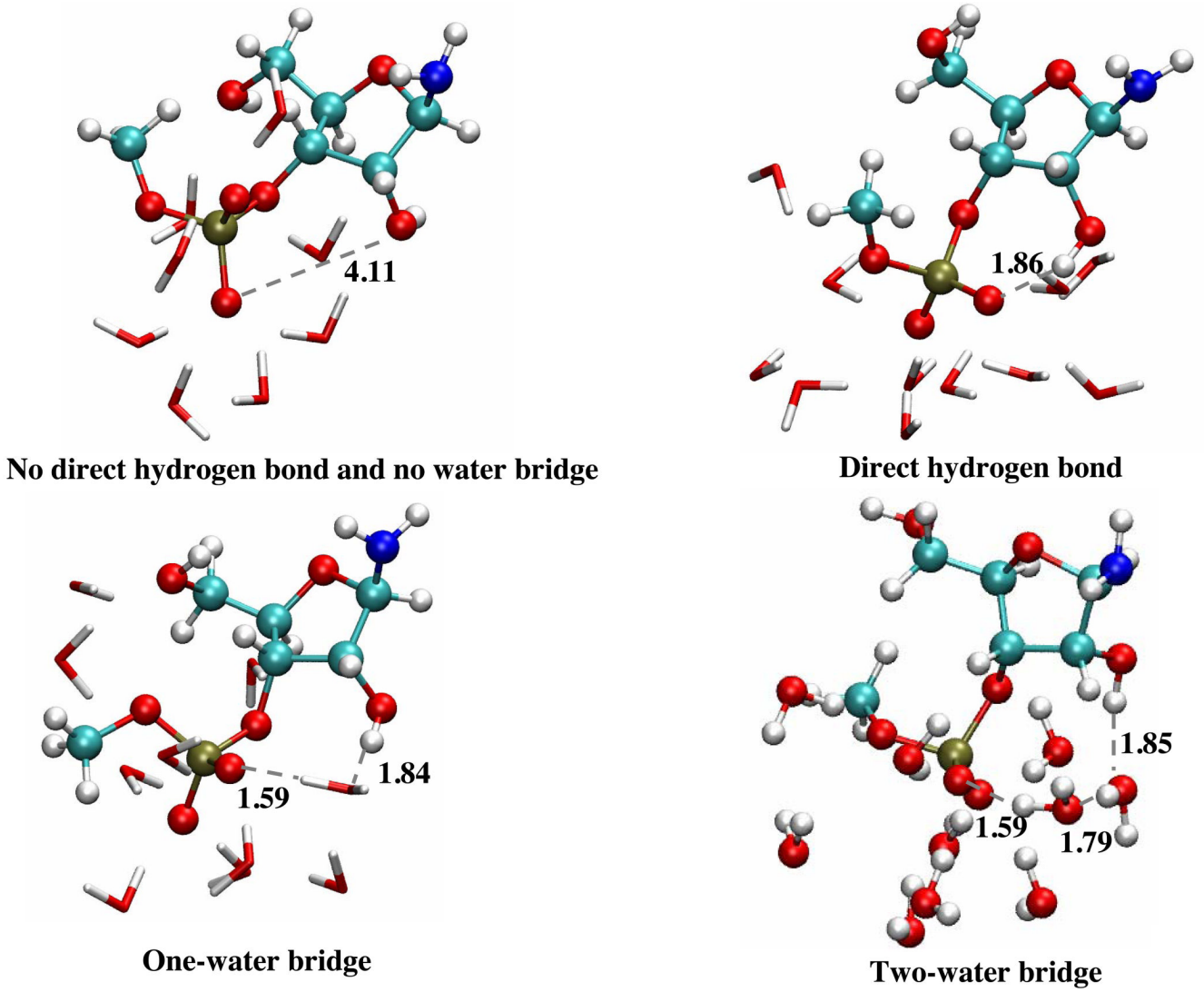

Figure 3.

Representative snapshot of the solute and nearby solvent configurations from the aqueous solution simulations. The snapshots illustrate different hydrogen bonding patterns involving the nucleophile (2'-OH), the phosphate group and nearby water molecules. Relevant hydrogen bonding distances (between hydrogen and acceptor atom) are given in Angstroms.

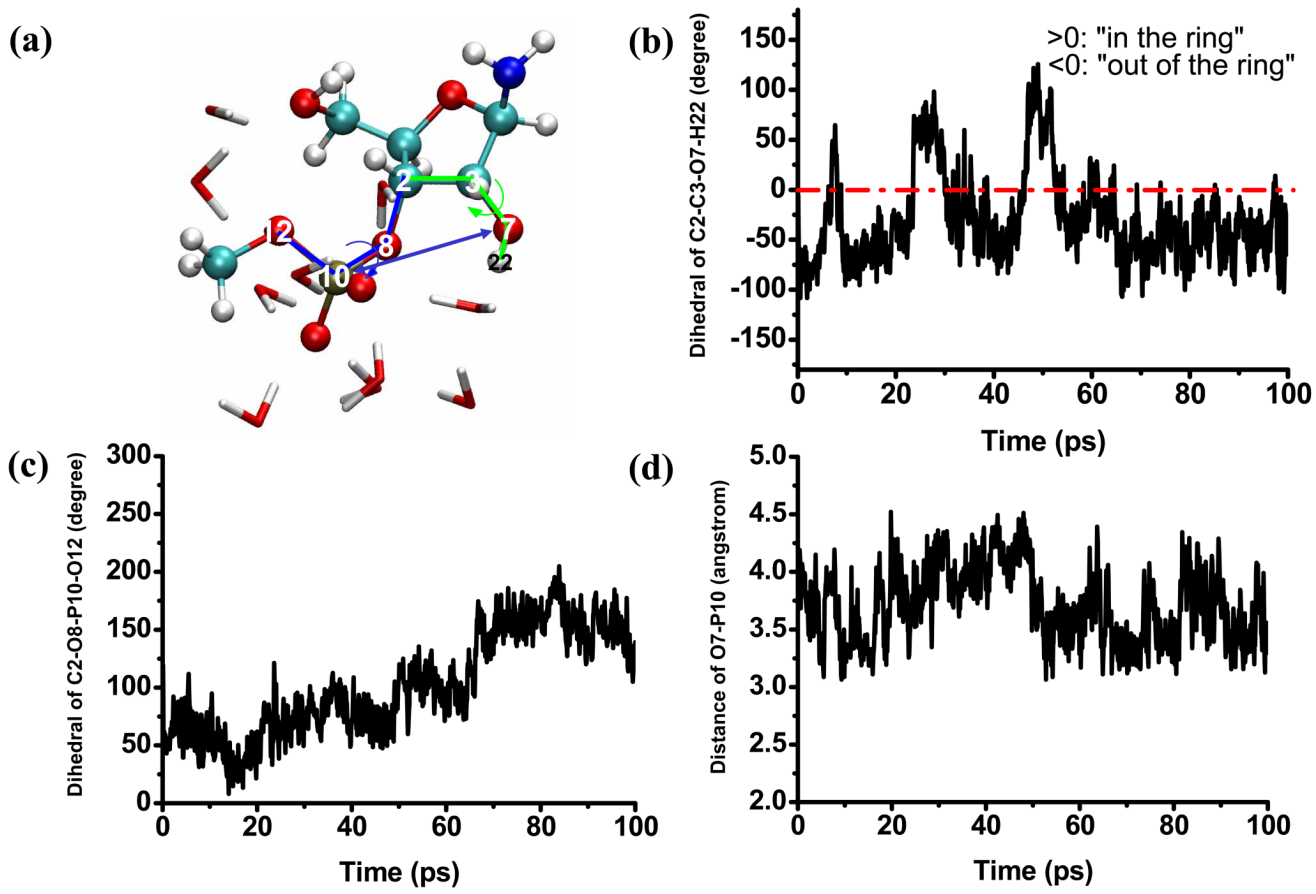

Figure 4.

Time dependence of several key geometrical parameters of the solute (indicated in a) during the aqueous solution simulations. These results illustrate the structural flexibility of the solution in the aqueous solution environment.

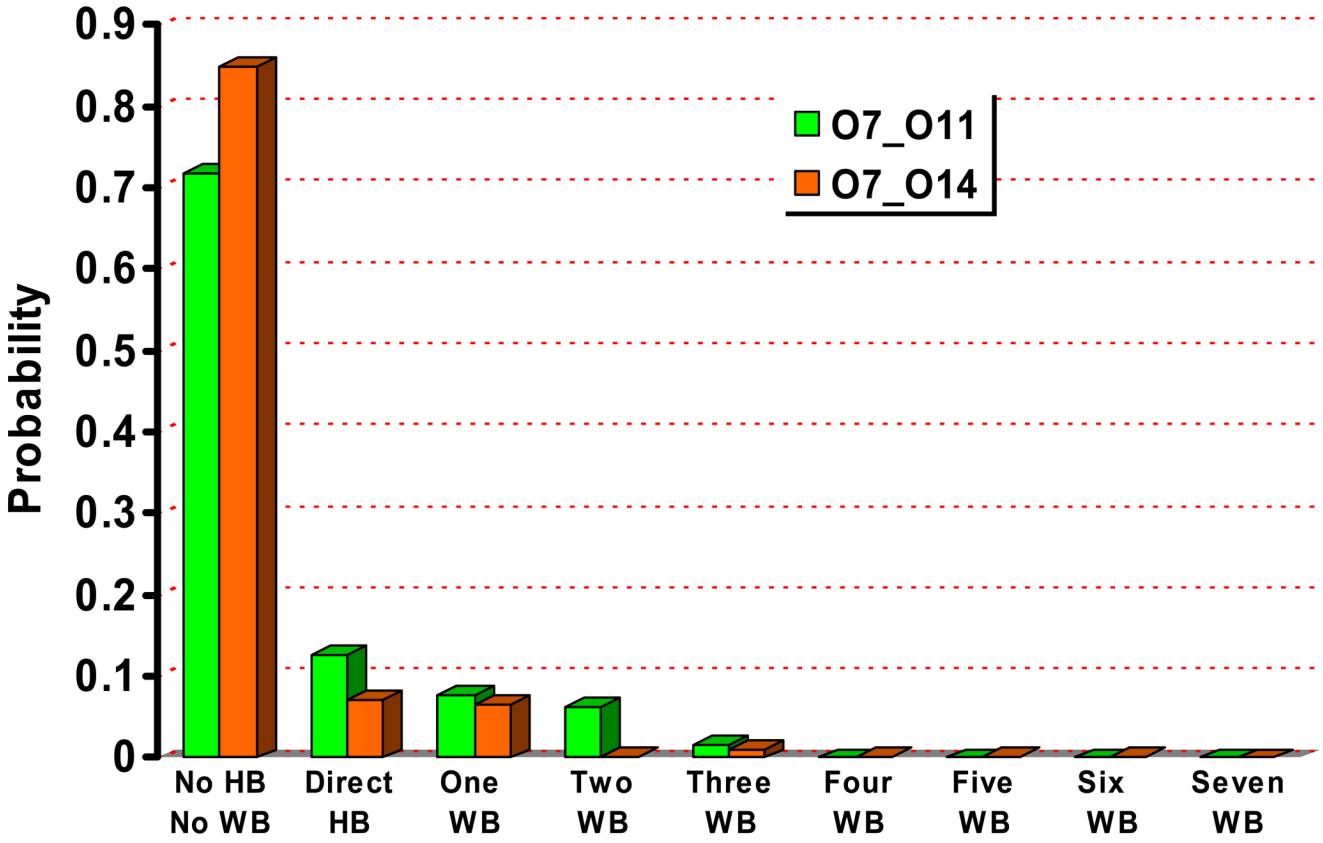

Figure 5.
Statistical analysis of the hydrogen bonding pattern associated with the nucleophile (2'-OH) and the phosphate group (either O_{11} or O_{14}, see Fig. 1 for labels) during the aqueous solution simulations. "No HB/No WB" indicates configurations in which the two groups are not engaged in either a direct hydrogen bond or indirect hydrogen bond through water molecules; "Direct HB" indicates a direct hydrogen bonding interaction between the two groups; "One/Two etc. WB" indicates that the two groups are connected through a specific number of bridging water molecules.

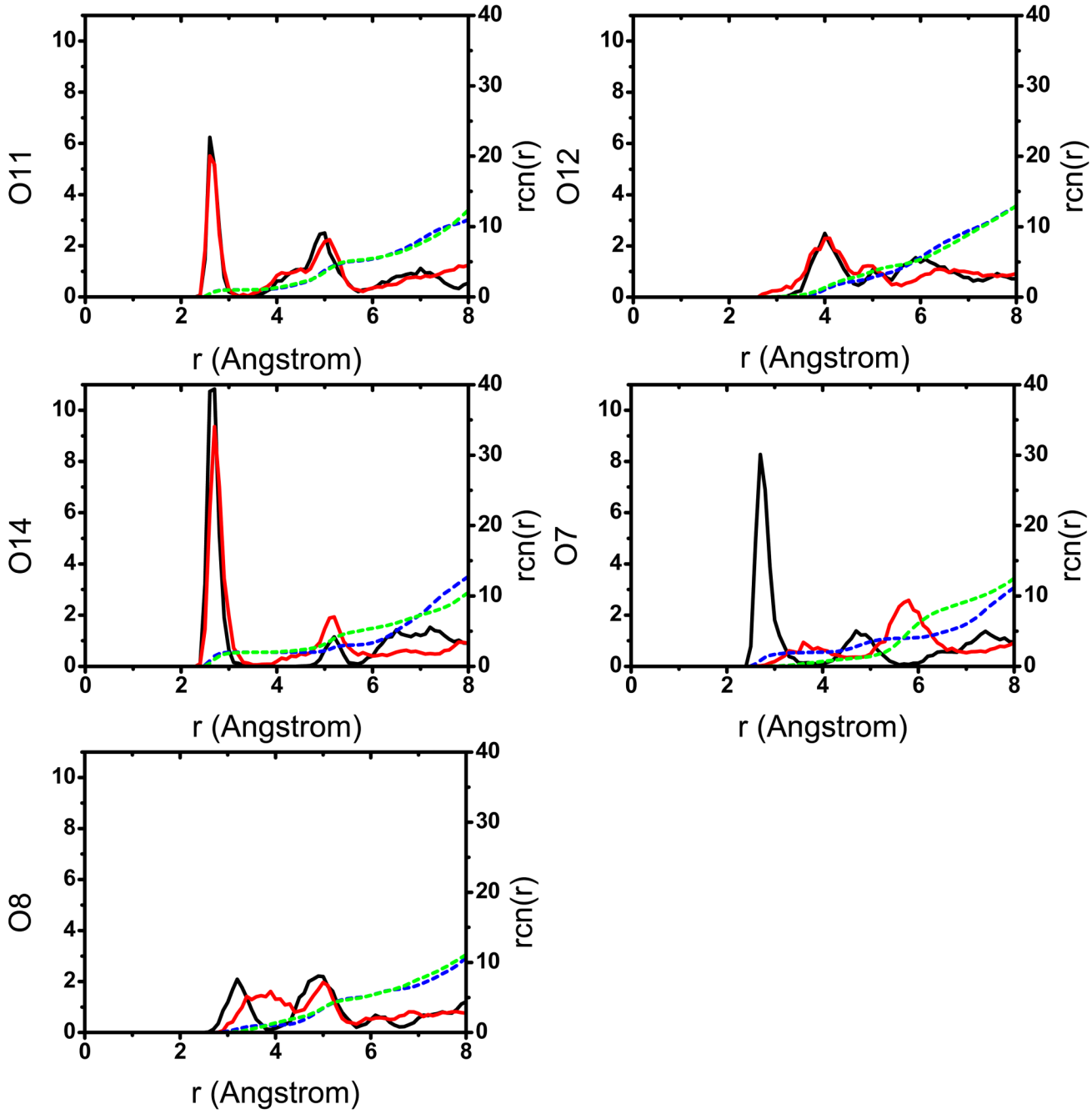

Figure 6.
Radial distribution functions, g(r) (solid lines) and running coordination numbers, rcn (dash lines), of *tert*-butanol oxygen around different oxygen atoms of UNP; black/blue and red/green represent results from two independent simulations.

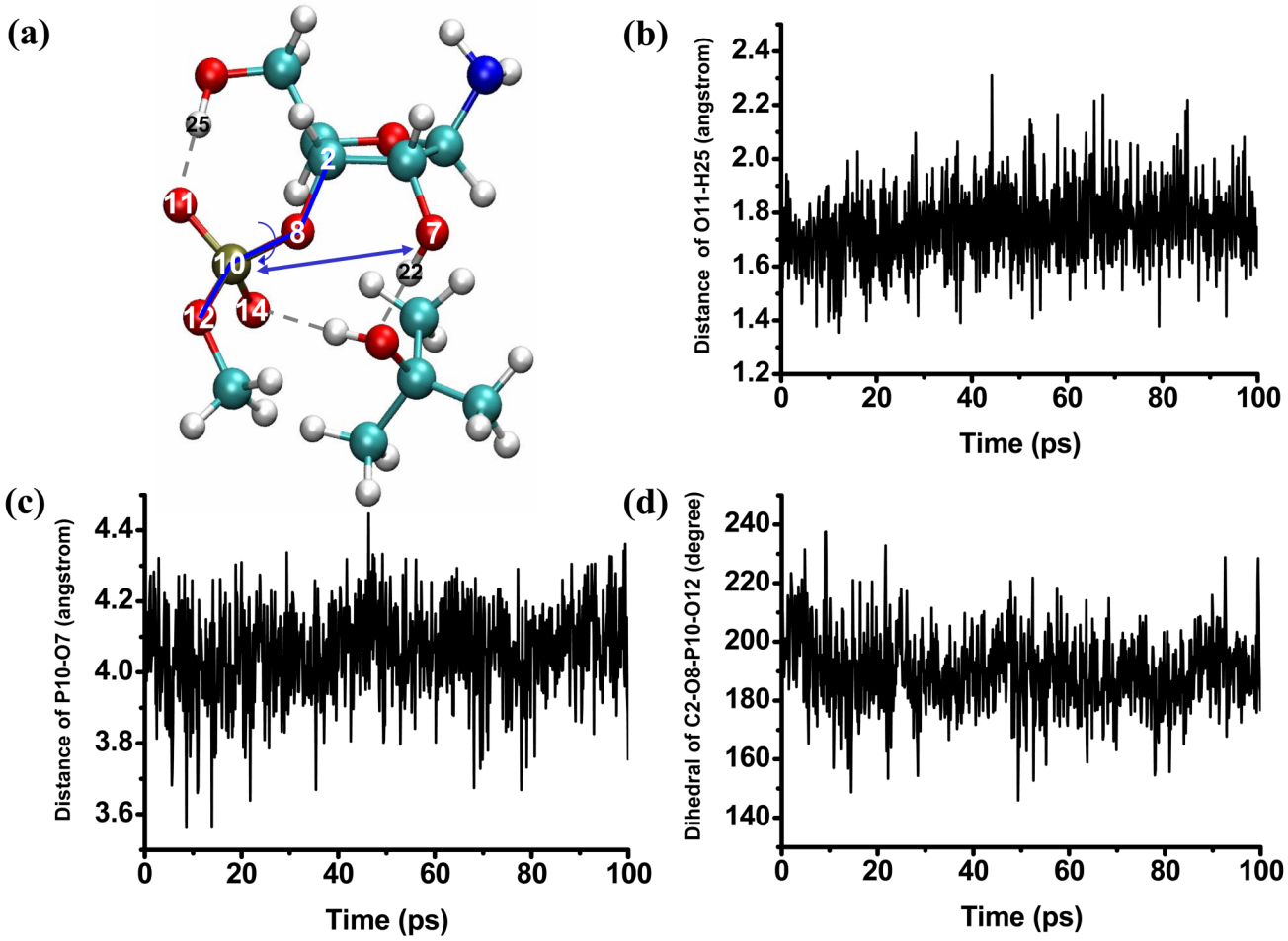

Figure 7.

Time dependence of several key geometrical parameters of the solute (indicated in a) during the first set of *tert*-butanol solution simulation; an intramolecular hydrogen bond involving the 5'-OH and the phosphate makes the phosphate and the 2'-OH far separated, allowing a *tert*-butanol solvent to insert in between. This configuration remains stable at least on the 300 picosecond time scale (data for the last 100 ps are shown).

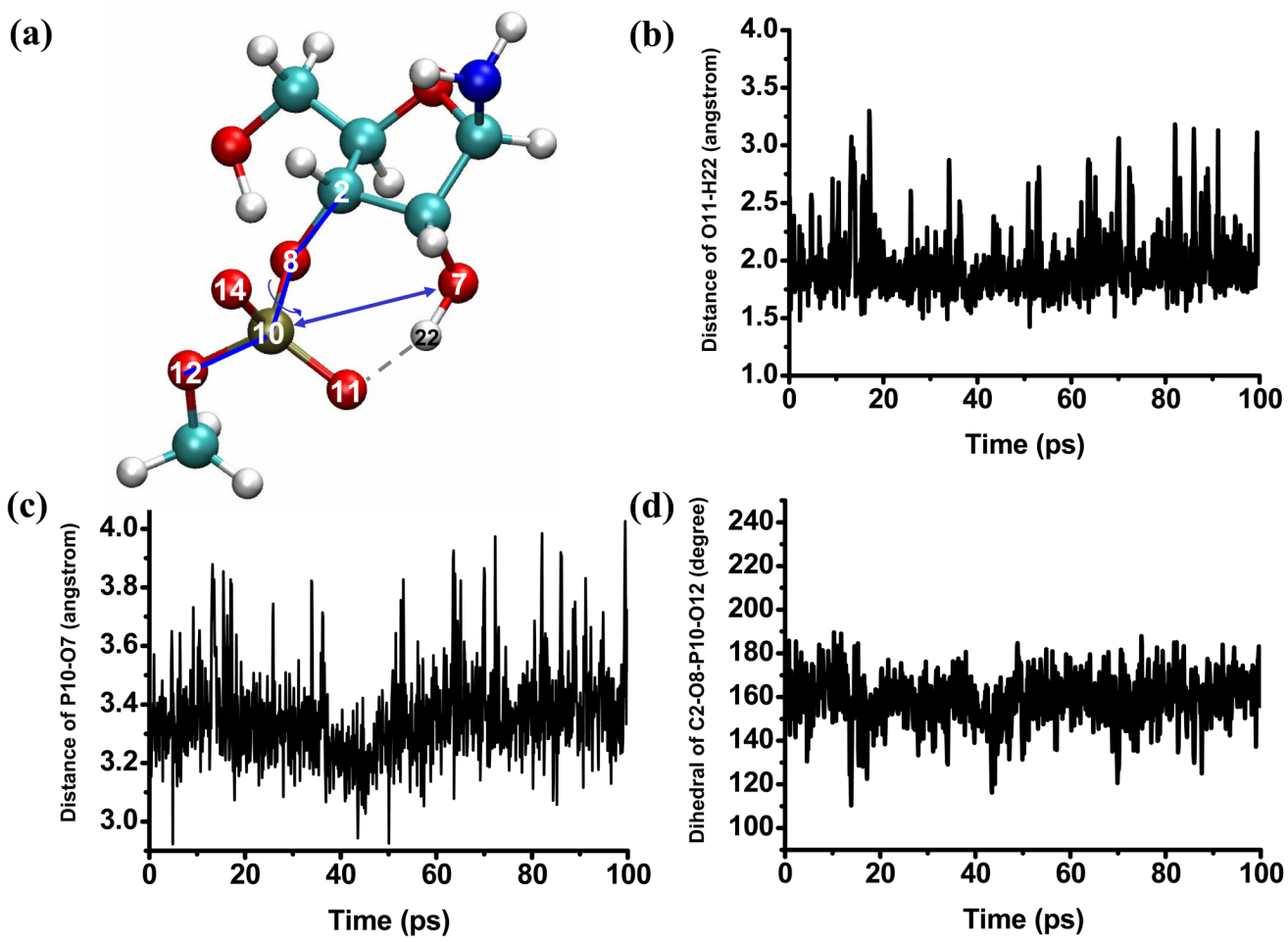

Figure 8.

Same as Fig.7, but from an independent trajectory starting from a different initial solute configuration. Here a direct hydrogen bond is formed between the nucleophile (2'-OH) and the phosphate and remains stable throughout the 300 ps simulation (data for the last 100ps are shown).

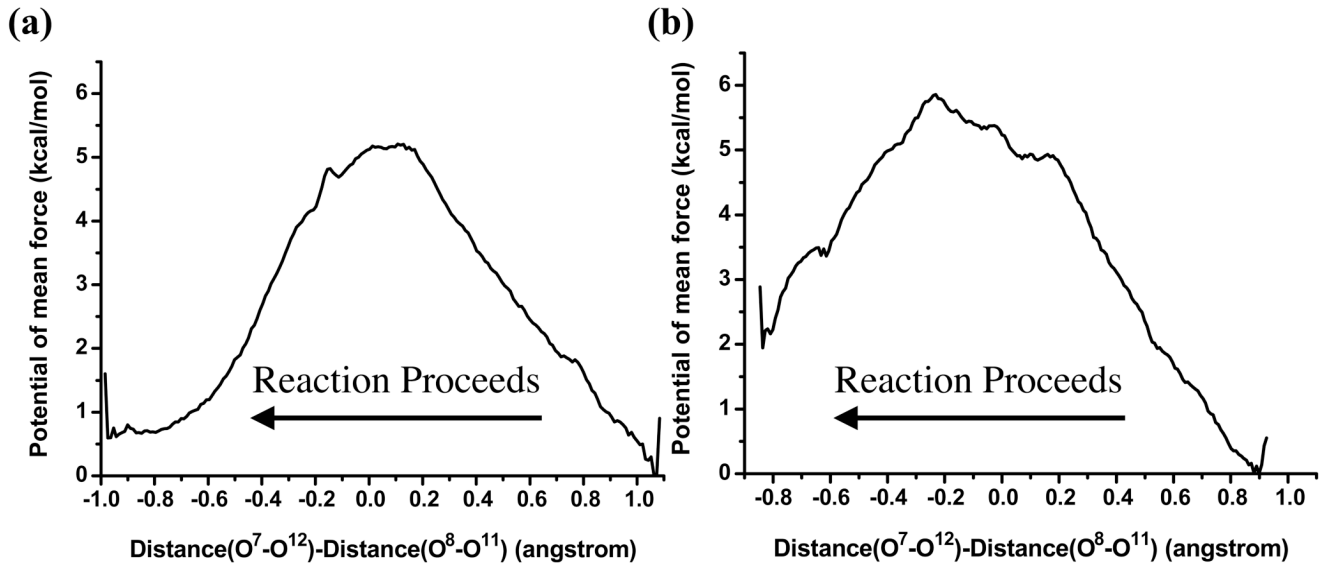

Figure 9.

One-dimensional potential of mean force (in kcal/mol) for the pseudo-rotation of the pentavalent intermediate in (a) aqueous solution and in (b) *tert*-butanol; the antisymmetric stretch defined as $d(O_7\text{-}O_{12})\text{-}d(O_8\text{-}O_{11})$ is used as the reaction coordinate (see text and Supporting Information for further discussions regarding the choice of the reaction coordinate).

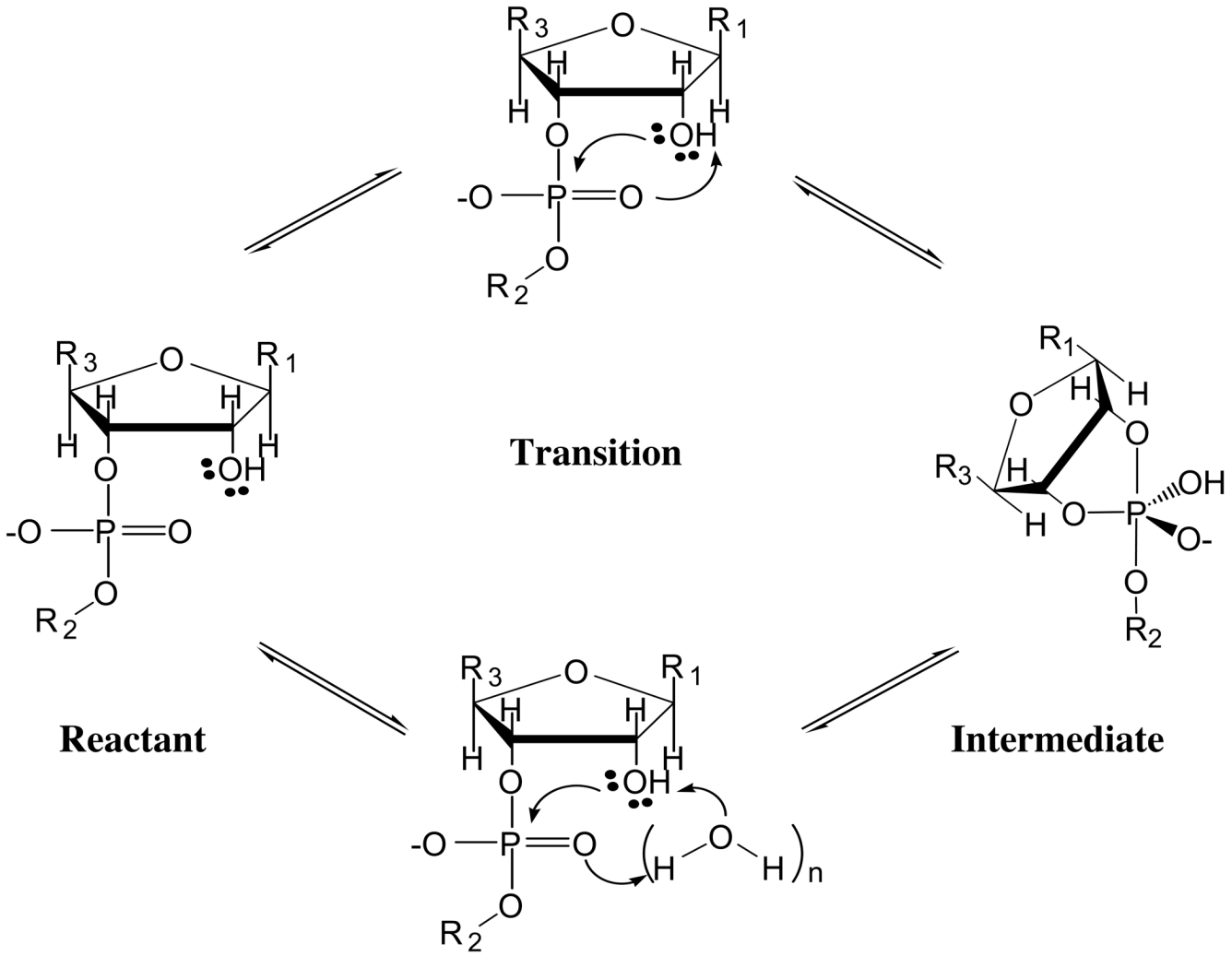

Scheme 1.
Relayed proton transfer through water molecules (or amino acid sidechains in enzymes) in phosphoryl transfer reactions illustrated using RNA as an example.

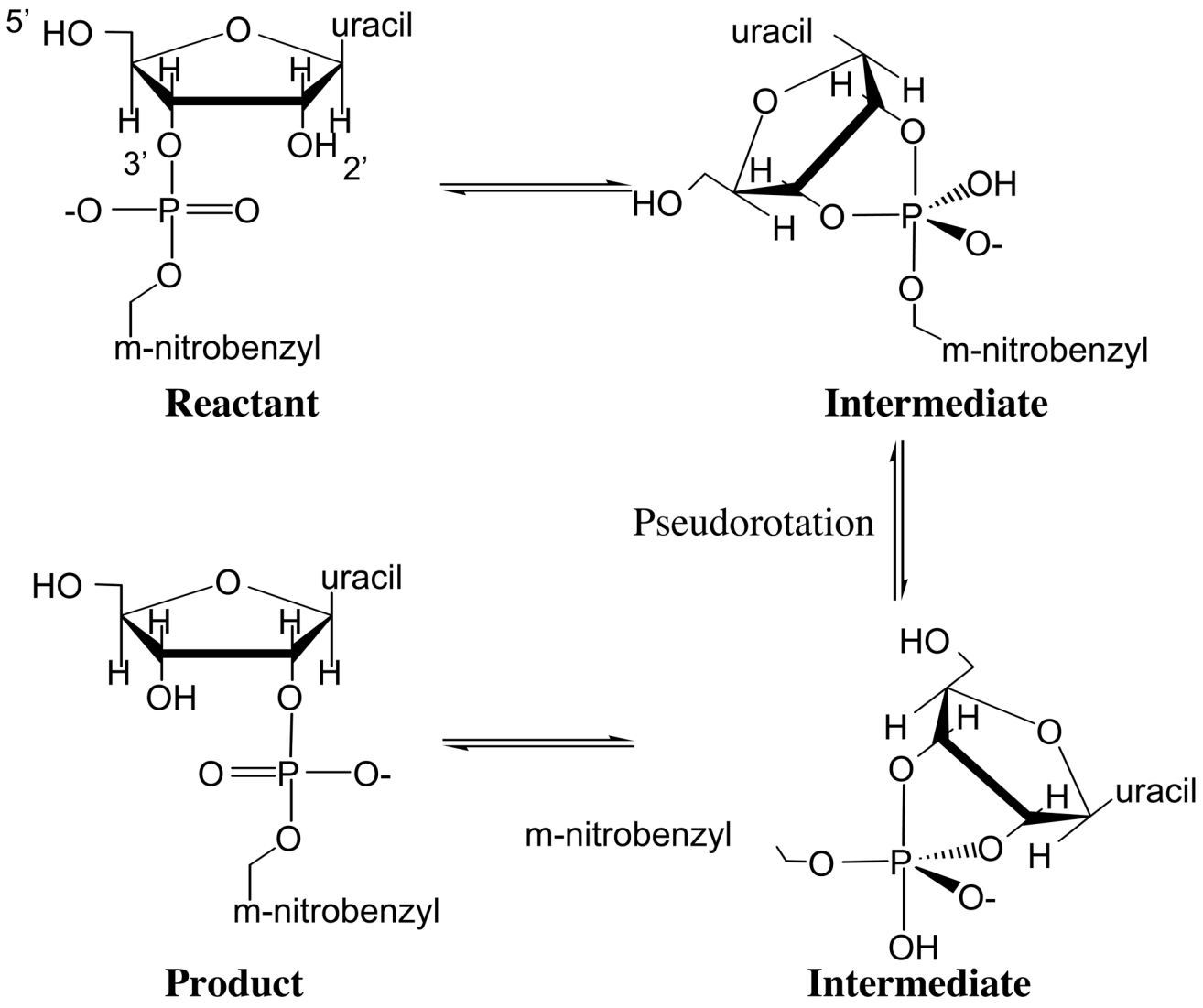

Scheme 2.
The reaction scheme for the isomerization of uridine 3’-m-nitrobenzyl phosphate (UNP).

Table 1

Geometrical parameters for the reactant and transition from Minimum Energy Path (MEP) analysis for the phosphoryl transfer reaction of model UNP with different hydrogen-bonding interactions between the nucleophile (2'-OH) and phosphate[a]

Geometrical Parameters[b]	DH	1W
$P\text{-}O_7$	3.396 (0.015)/2.270 (0.100)	4.140 (0.042)/2.900 (0.199)
$P\text{-}O_{12}$	1.646 (0.001)/1.670 (0.008)	1.665 (0.014)/1.635 (0.012)
$P\text{-}O_8$	1.696 (0.005)/1.665 (0.014)	1.670 (0.017)/1.621 (0.010)
$P\text{-}O_{11/14}$	1.517 (0.004)/1.636 (0.009)	1.515 (0.004)/1.600 (0.005)
$H_{22}\text{-}O_7$	0.994 (0.001)/1.742 (0.040)	0.989 (0.001)/1.578 (0.029)
$H_{22}\text{-}O_{11/14}$	1.781 (0.011)/0.989 (0.006)	N/A
$\angle O_7\text{-}P\text{-}O_{12}$	126.5 (0.6)/162.1 (1.3)	124.3 (5.0)/156.0 (4.1)
$\angle O_7\text{-}H_{22}\text{-}O_{11/14}\text{-}P$	35.6 (0.5)/−1.2 (2.0)	N/A
$H_{22}\text{-}O_W$	N/A	1.867 (0.059)/1.019 (0.007)
$H_W\text{-}O_W$	N/A	1.000 (0.004)/1.953 (0.075)
$H_{W'}\text{-}O_{11/14}$	N/A	1.727 (0.059)/0.993 (0.001)

a) The results are averaged over snapshots collected from aqueous solution simulations that include either a direct hydrogen bond (DH) between the nucleophile and phosphate or a single bridging water molecule (1W). The numbers without parentheses are the average values and those with parentheses are standard deviations (9 snapshots for DH and 7 snapshots for 1W). All structures have been optimized at the B3LYP/6–31+G* level in the gas phase. Values before the slash are for the reactant state, and those after the slash are for the transition state.

b) Distances are in angstrom; angle and dihedral angles are in degrees. For labels of atoms, see Fig. 1; the subscript "W" indicates the bridging water in 1W cases, and $O11/14$ means either $O11$ or $O14$, whichever acts as the proton acceptor during the nucleophilic attack.

Table 2

Results from Minimum Energy Path (MEP) analysis for the phosphoryl transfer reaction of model UNP with different hydrogen-bonding interactions between the nucleophile (2'-OH) and phosphate[a]

State	Gas phase 6–31+G* OPT[b]	Gas phase 6–311++G** SP[b]	PCM 6–311++G** UAKS SP[b]	PCM 6–311++G** Pauling SP[b]
Reactant (DH)	0.0/0.0	0.0/0.0	0.0/0.0	0.0/0.0
TS (DH)	30.0 (1.0) /29.2 (0.5)	29.7 (0.8)/28.9 (0.4)	26.1 (2.5)/24.7 (2.3)	28.0 (1.3)/26.6 (1.2)
INT (DH)	28.6 (0.9)/28.5 (0.7)	29.1 (0.8)/28.9 (0.7)	21.2 (0.6)/20.6 (0.5)	25.5 (0.4)/24.8 (0.2)
Reactant (1W)	0.0/0.0	0.0/0.0	0.0/0.0	0.0/0.0
TS (1W)	28.9 (2.1)/27.4 (1.6)	28.3 (2.0)/26.8 (1.4)	26.1 (2.4)/24.1 (2.4)	26.5 (1.6)/24.5 (1.6)
INT (1W)	28.1 (2.6)/27.1 (1.8)	27.5 (2.4)/26.5 (1.7)	25.6 (2.9)/23.5 (3.0)	25.6 (2.5)/23.6 (2.7)

*c)*The energetics are given relative to the respective reactant state in kcal/mol; the values before the slash are potential energies, those after the slash are Gibbs free energies calculated at 300 K using the harmonic-oscillator-rigid-rotor model. The results are averaged over snapshots collected from aqueous solution simulations that include either a direct hydrogen bond (DH) between the nucleophile and phosphate or a single bridging water molecule (1W). The numbers without parentheses are the average values and those with parentheses are standard deviations (9 snapshots for DH and 7 snapshots for 1W).

*d)*The structures have been optimized (OPT) at the B3LYP/6–31+G* level; the vibrational contributions are also calculated at this level of theory. Single point (SP) calculations are then carried out with the 6–311+G** basis set in either the gas-phase or solution using the PCM model (either UAKS or Pauling radii).